A TWO-STEP PROCEDURE FOR HAZARD PREDICTION AND ASSESSMENT OF LANDSLIDE AND DEBRIS FLOW

Chunxiang Wang[1], Hideaki Marui[2], Gen Furuya[3] and Naoki Watanabe[4]

ABSTRACT

Landslides and debris flows, the main types of movements when slope failures occur, are sources of severe geohazards in mountainous regions throughout the world. Most debris flows originally occur in the form of rainfall-induced landslides before they move into valley channel. In this paper, a two-step procedure to define landslide and debris flow susceptibility in a mountainous region has been attempted. Firstly, a GIS-based three-dimensional limit equilibrium stability analysis model is used to define the potential landslides. Then, using GIS-based two-dimensional numerical simulation model of debris flow, the inundated area across three-dimensional terrain is defined; and the potentially affected homes, streams and road sections are predicted. The application to the region of Minamata-Hougawachi, Kumamoto Prefecture in Japan has indicated that the present proposal is effective for landslide hazard mapping and risk analysis. The reliable results, simplified scenario studies and the possibilities of visualization will help increase the acceptance of hazard maps and improve ways for dealing with the risk of landslide and debris flows.

Keywords: Landslide, Debris flow, Geographic Information System (GIS), Numerical model, Hazard, Assessment

INTRODUCTION

Landslides and debris flows constitute one of the more important natural hazards throughout the world. Landslide occurrence and reactivation is conditioned by a number of terrain and geo-environmental factors such as rock and soil properties, weathering, jointing and structure, slope morphology, land cover/use, and underground water flow. Landslides can be triggered by many natural phenomena such as earthquake, heavy or prolonged rainfall and snow melt. Analyzing the relationship between landslides and the various factors causing landslides not only provides an insight to understand of landslide mechanisms, but also can form a basis for predicting future landslides and assessing the landslide hazard. Therefore, the study of the mechanisms and properties of past landslide is a valuable reference for assessing the future landslide hazard in its adjacent or geotechnically similar area.

Most debris flows originally occur in the form of rainfall-induced landslides before they move into valley channel (Fleming et al., 1989; Wen and Aydin, 2005). Slides that mobilize into flows usually are characterized by high-velocity movement and long run out distance and may present the greatest risk to human life. Strategies should be devised to help understand landslide processes, analyze threatening landslide hazard and predict future landslides in order to reduce ongoing and future damage from landslides. Therefore, prediction of the inundated area, including the potentially affected inhabited areas, is of great importance in debris flow risk assessment.

On July 19-20, 2003, a short duration high intensity rainfall event impacted the city of Minamata in Kumamoto prefecture, Japan. This rainfall triggered many landslides and debris flows (Iwao, 2003; Taniguchi, 2003). The slope failure and resultant debris flow at Hogawachi in Minamata was the

[1] Assoc. Prof. Chunxiang Wang. Research Institute for Natural Hazards and Disaster Recovery, Niigata University (e-mail: chunxiangwang@hotmail.com)
[2] Prof. Hideaki Marui. Research Institute for Natural Hazards and Disaster Recovery, Niigata University
[3] Assoc. Prof. Gen Furuya. Research Institute for Natural Hazards and Disaster Recovery, Niigata University
[4] Assoc. Prof. Naoki Watanabe. Research Institute for Natural Hazards and Disaster Recovery, Niigata University

largest and most damaging of these disasters (Fig.1). A moderatesized, 4-9m deep debris avalanche triggered the debris flow about 1.5 km upslope of where the casualties occurred. The volume of sediment discharge plunging into the village of Minamata-Hougawachi, was estimated about 1,000,000 m^3, and the velocity of debris flow was estimated from about 2.9m/s to 23.5 m/s (Taniguchi, 2003). The disaster killed 15 people and more than 14 houses were either damaged or destroyed.

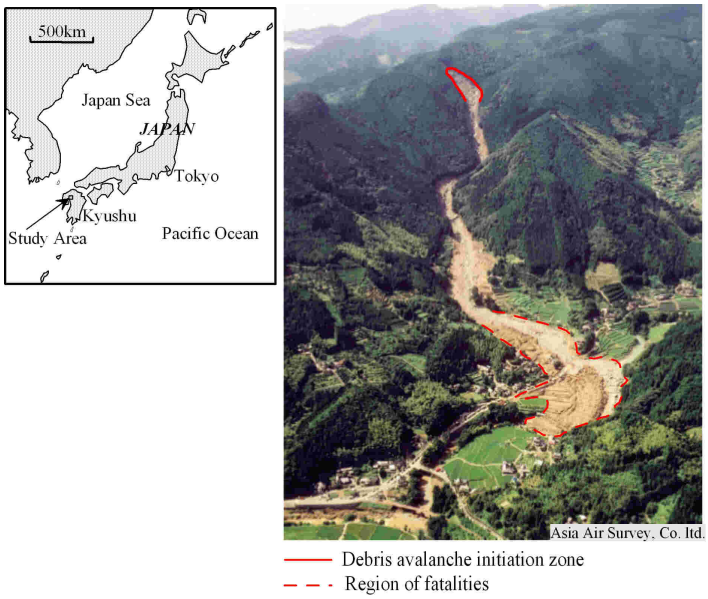

Fig.1 The 20 July 2003 debris flow disaster at Hougawachi, Kumamoto Prefecture, Japan

In this disaster, the types of movement of soil and rock material are sliding and flow. In this study, a two-step procedure to define landslide and debris flow susceptibility in a mountainous region has been presented (Fig.2). Firstly, a GIS-based three-dimensional limit equilibrium stability analysis model (Xie et al., 2003) is used to define the potential landslides. Then, using GIS-based two-dimensional numerical simulation model of debris flow (Wang et al., 2008), the inundated area across three-dimensional terrain is defined; and the potentially affected homes, streams and road sections are predicted.

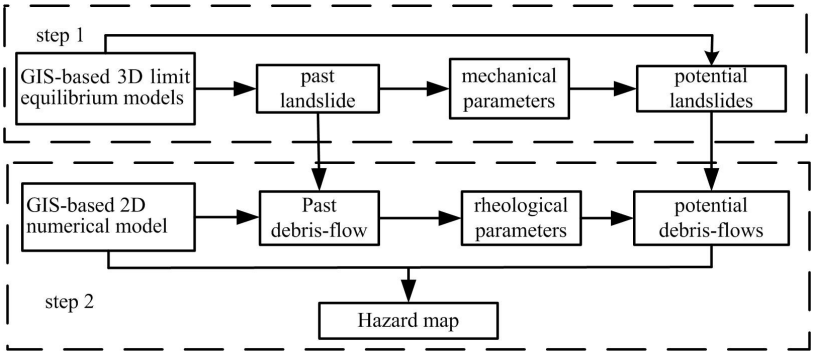

Fig.2 Approaches for regional slope-failure hazard

ANALYSIS OF THE HISTORIC LANDSLIDE

The slope failure occurred at 4:20 am on July 20, 2003, 4.3 hours after the beginning of the rainstorm and during the period of highest rainstorm intensity (Fig.3). The soil stratigraphy at the landslide site is schematically illustrated in Fig.4. The landslide mass can be considered to have been triggered by a rapid increase in the pore water pressure. The landslide mechanism was controlled by local lithological conditions where an almost impermeable layer (An-5: tuff breccia, brecciated lava, and lava) is overlaid by highly weathered rock (An-7, mainly lava with subordinate tuff breccia) (Fig.4). During the intense rainfall, high pore water pressure likely developed at the base of the weathered An-

7 within the limited space in the fractures and interstices. Field surveys have indicated that almost no subsurface water infiltrated the exposed bedrock one week after the landslide, demonstrating the rapid accretion of pore pressure in the weathered regolith during the rainstorm. The landslide mass developed into debris flow after it entered the stream channel and impacted the village after traveling about 1.5km in 3 minutes (Fig.1).

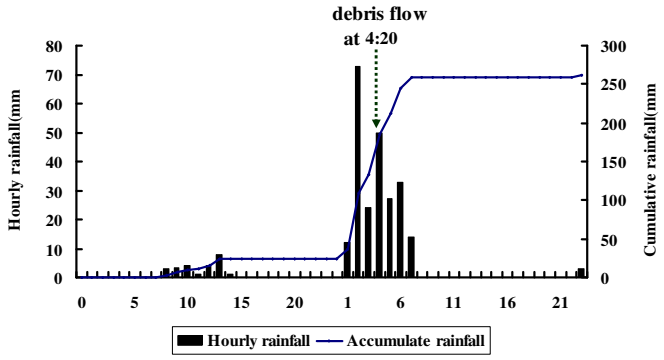

Fig.3 Precipitation at Minamata City (July 19 0:00 to July 20 22:00, 2003)

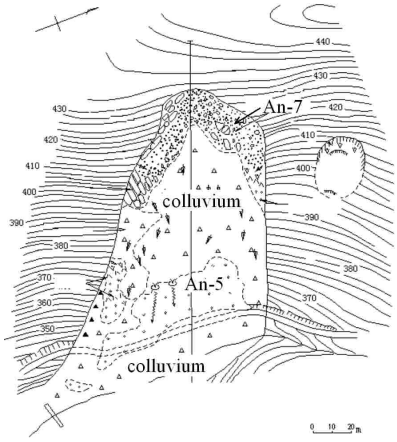

Fig.4 Schematics of the landslide mass

LANDSLIDE SUSCEPTIBILITY MAP

THE STUDY AREA

As the adjacent region has similar engineering geological conditions, we assume that the slope failure in this region has the same mechanism with the past landslide. In an attempt to forecast a similar landslide related disaster in the future, this study will concentrate on landslide hazards around the site of the July 19-20 Minamata-Hougawachi landslide. Figure 5 shows the 2.5km by 3km study area, the local drainage system and the location of main roads and houses. The study area is limited to the region that containing map units An-7 and An-5(Fig. 6).

BASIC DATA

Based on a topographic map with a scale of 1:2500, a contour line file was generated, with a contour interval of 2m. This file was converted to a TIN (Triangulated Irregular Network) and subsequently a DEM (Digital Elevation Model). The roads and streams that located in the study area were stored as polylines, and the houses as polygons.

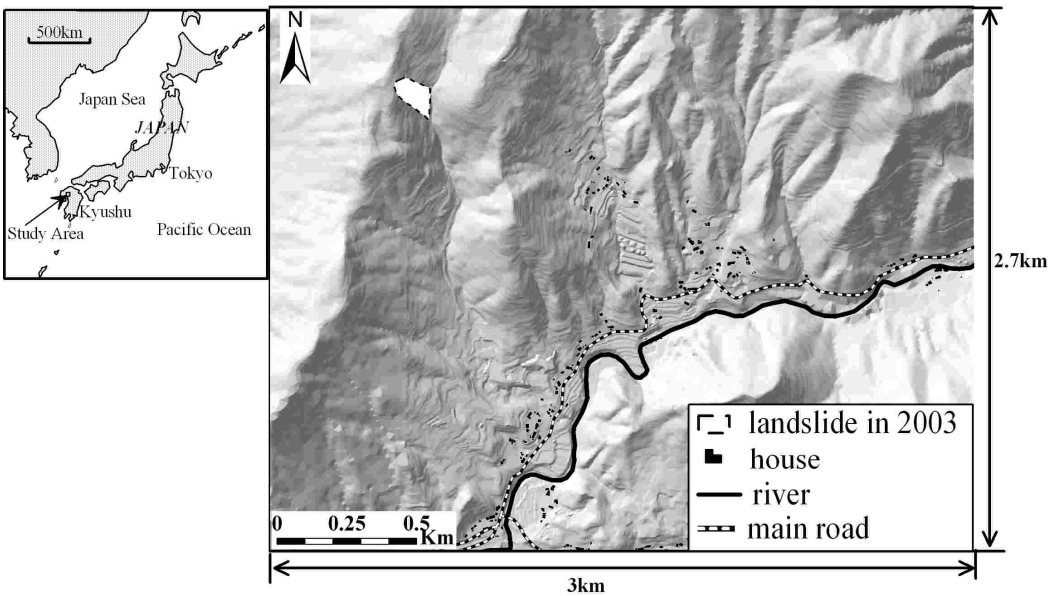

Fig.5 Study area with distribution of houses, river and main road

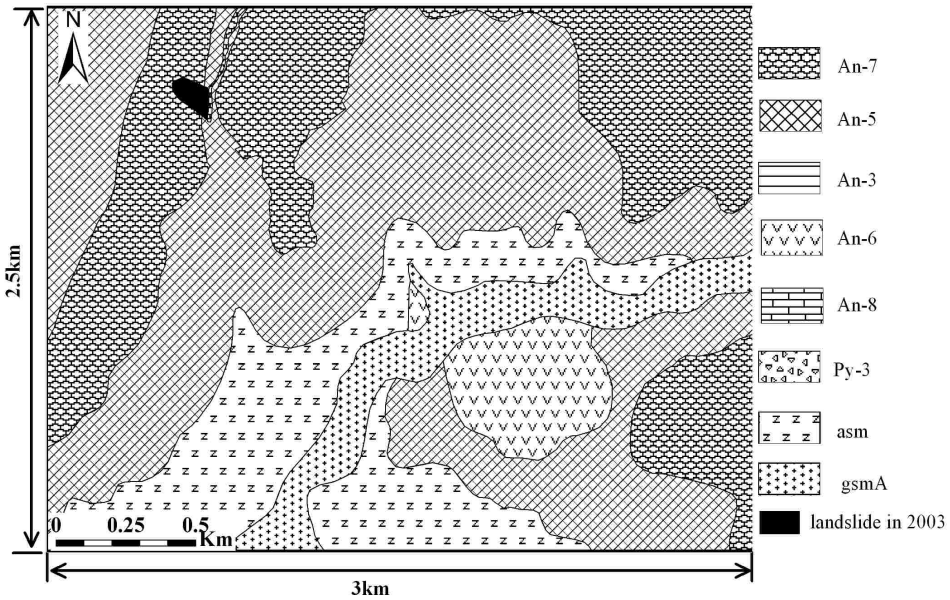

Fig.6 Lithological map of the study area (An-3: Andesitic rock-3 (tuff breccia, brecciated lava, and lava); An-5: Andesitic rock-5 (tuff breccia, brecciated lava, and lava); An-6: Andesitic rock-6(neck); An-7: Andesitic rock-7 (mainly lava with subordinate tuff breccia); An-8: Andesitic rock-8 (lava); Py-3: pyroclastics-3; Asm: Alternating beds of sandstone and mudstone; gsmA: gravel, sand and mud (lowland sediments))

SLOPE UNITS

For the landslide hazard assessment of a large mountainous area with complex geometry and geological conditions, a key problem is how to extract the appropriate slope unit for potential sliding surface identification and minimum 3D safety factor calculation. Slope unit, namely, the portion of land surface delimited by watershed divides and channels has similar topographic and geological characteristics. The suitability of the slope-units for landslide hazard assessment and for other land-related study has been recognized by several authors (Hansen, 1984; Carrara et al., 1991; Dymond et al., 1995).

A GIS-based hydrologic analysis and modeling tool, Arc Hydro (David, 2002), is employed to draw watershed divides and to delineate slope units automatically from a DEM (Fig.7) over this geologically similar study area.

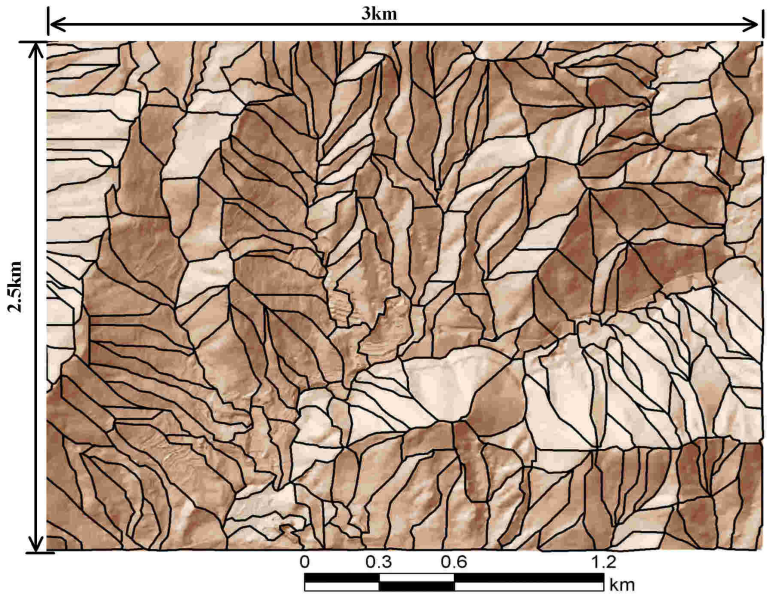

Fig.7 Distribution of slope units

ANALYSIS OF MECHANICAL PARAMETERS

Based on the field landslide survey of July 20, 2003, the geometry of the landslide was described (Fig. 4). The engineering geological report of this area provided several pairs of mechanical parameters (Tab.1). In order to determine one pair to represent the shear parameters of the sliding surface, using the geometry information in Fig. 4 and the GIS-based 3D limit equilibrium models (Revised Hovland model, 3D extension of Bishop model and 3D extension of Janbu model) (Xie et al., 2003, 2006), the 3D safety factor with different pairs of shear parameters is calculated (Tab.1).

Revised Hovland model is

$$SF_{3D} = \frac{\sum_j \sum_i \left(cA + (W+P)\cos\theta \tan\phi\right)\cos\theta_{Avr}}{\sum_j \sum_i (W+P)\cos\theta_{Avr}\sin\theta_{Avr}} \tag{1}$$

3D extension of Bishop model is

$$SF_{3D} = \left(\sum_j \sum_i (W+P)\sin\theta_{Avr}\right)^{-1} \sum_j \sum_i \frac{(W+P)\tan\phi + cA\cos\theta}{\cos\theta + SF_{3D}^{-1}\tan\phi\sin\theta_{Avr}} \tag{2}$$

and 3D extension of Janbu model is

$$SF_{3D} = \frac{\sum_j \sum_i [cA + N\tan\phi]\cos\theta_{Avr}}{\sum_j \sum_i N\sin\theta\cos(\theta_{Asp} - \theta_{AvrAsp})}, \quad N = \frac{P + W - SF_{3D}^{-1}cA\sin\theta_{Avr}}{\cos\theta + SF_{3D}^{-1}\tan\phi\sin\theta_{Avr}} \tag{3}$$

where, SF_{3D} is the 3D slope safety factor; W is the weight of one column; A is the area of the slip surface; P is the vertical force acting on each column (the distributed force of upper load), here $P = 0$; N is the normal force on each column; c is the cohesion; ϕ = the friction angle; θ is the dip (the normal angle of slip surface); θ_{Avr} is the apparent dip in the main inclination direction of the slip surface; θ_{Asp} is the dip direction of the grid column slip surface; θ_{AvrAsp} is the average dip direction of the slip surface; and j and i are the numbers of row and column of the grid in the range of slope failure.

By analyzing the results where the 3D safety factor is less than 1 (Tab. 1), the parameters of c=20 kn/m^2 and ϕ=26° were chosen to represent the shear parameters of the sliding surface. These parameters will be used in the slope stability analysis of the adjacent region.

Tab.1 Mechanical parameters and safety factors

case (**c: kn/m^3**)	3D Safety Factor		
	Revised Hovland model	3D extension of Bishop model	3D extension of Janbu model
c = 20, ϕ=23°	0.801	0.834	0.786
c = 21, ϕ=26°	0.949	0.981	0.903
c = 19, ϕ=26°	0.801	0.839	0.768
c = 23, ϕ=33°	1.102	1.159	1.059
c = 19, ϕ=25°	0.830	0.867	0.795
c = 22, ϕ=25°	0.978	1.010	0.931
c = 21, ϕ=31°	0.955	1.006	0.919
c = 24, ϕ=30°	1.132	1.177	1.081

DISTRIBUTION OF POSSIBLE LANDSLIDES

As the adjacent region has similar engineering geological conditions, we assume that the slope failure in this region has the same mechanism with the past landslide, that is to say, the potential failure surface would develop along the interface between map units An-5 and An-7 under heavy rainfall. To detect the 3D critical slip surface of each slope unit, a search is performed by Monte Carlo simulation. The initial slip surface is assumed to be the lower part of an ellipsoid and changes according to multiple layer strengths and the conditions of the discontinuous surface. The five parameters that describe an ellipsoid are selected as random variables with uniform distribution: three axial

parameters “a, b, c”, the central point “C”, and the inclination angle “θ” of the ellipsoid (Fig. 8). The central point of the ellipsoid is first set as the central point of a slope unit, and then randomly chosen within a certain range. The critical slip surface is fulfilled by searching the parameter space of the 3D safety factor. If a randomly produced slip surface is lower than the interface of map units An-7 and An-5, it is limited by the interface itself.

Using the same engineering geological conditions of the past landslide, and the same triggering factor (rainstorm), the minimum 3D safety factor is calculated for each slope unit. Since a single value of safety factor is not sufficient enough for evaluating the slope stability of a slope unit, the ratio of the number of safety factor values less than 1.0 to the total times of calculation is calculated as the failure probability of the slope unit. If the failure probability is more than 80%, the slope unit is clarified as unstable (Fig. 9).

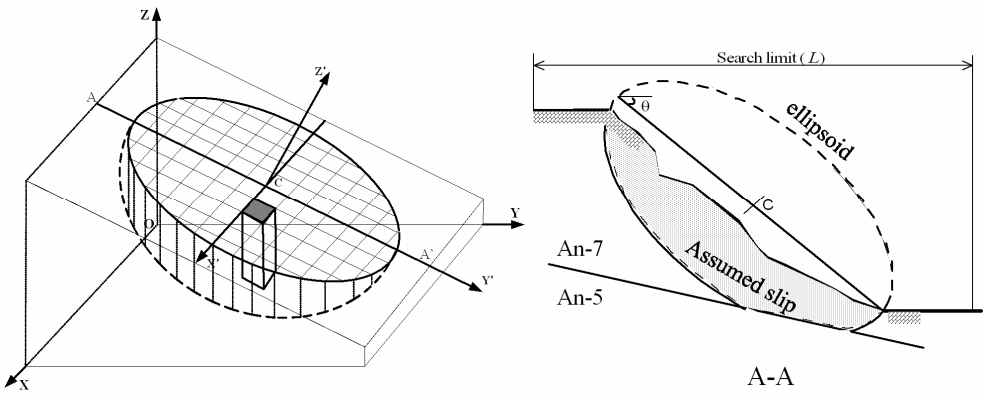

Fig.8 Example of randomly produced ellipsoid used to simulate the 3D slide mass

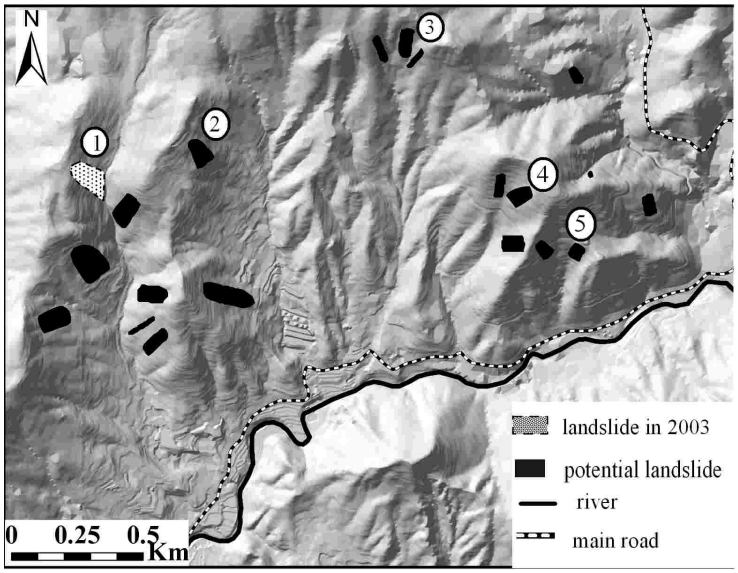

Fig.9 Distribution of the past landslide and the 19 potential landslides
(case 1: landslide in 2003; cases 2-5: for prediction)

TWO-DIMENSIONAL NUMERICAL MODEL OF DEBRIS FLOW

Debris flows are rapidly flowing mixtures of water, clay, and granular materials and often are mobilized from rainfall-induced landslide (Mainali and Rajaratnam, 1994; Anderson, 1995; Fiorillo and Wilson, 2004; Fleming et al., 1989; Wen and Aydin, 2005; Dai et al., 1999). The key requirements in the assessment of debris flow risk consist of the predication of the flow trajectory over the complex topography, the potential runout distance and the inundation area in order to define a safety zone. Numerical simulation models incorporating GIS are important prediction tools.

GOVERNING EQUATIONS

Based on the conservation of mass and the momentum of the flow, many authors have proposed mathematical models of the debris flow, some of them are two-dimensional (Takahashi et al., 1992; O'Brien et al., 1993; Chen and Lee, 2000; Ghilardi et al., 2001; Denlinger and Iverson, 2001). The rainfall-induced debris flow is often considered to move as a continuous fluid until stoppage rather than as a sliding solid (Takahashi et al., 1992; Hunt, 1994; Hungr, 1995; Laigle and Coussot, 1997). The debris and water mixture is assumed to be uniform continuous, incompressible, unsteady Newtonian fluid. The derived equations using depth-averaged method to simulate the debris flow (Wang et al., 2008) are as following.

The continuity equation is

$$\frac{\partial h}{\partial t}+\frac{\partial M}{\partial x}+\frac{\partial N}{\partial y}=0 \tag{4}$$

And the momentum equations are

$$\frac{\partial M}{\partial t}+\alpha\frac{\partial (MU)}{\partial x}+\alpha\frac{\partial (MV)}{\partial y}=-\frac{\partial H}{\partial x}gh+\upsilon\beta\left(\frac{\partial^2 M}{\partial x^2}+\frac{\partial^2 M}{\partial y^2}\right)-\mu\sqrt{gh}\cos\theta_x\tan\xi \tag{5}$$

$$\frac{\partial N}{\partial t}+\alpha\frac{\partial (NU)}{\partial x}+\alpha\frac{\partial (NV)}{\partial y}=-\frac{\partial H}{\partial y}gh+\upsilon\beta\left(\frac{\partial^2 N}{\partial x^2}+\frac{\partial^2 N}{\partial y^2}\right)-\mu\sqrt{gh}\cos\theta_y\tan\xi \tag{6}$$

where $M = Uh$ and $N = Vh$ are the x and y components of the flow flux; U and V are the x and y components of the depth-averaged velocity; H is the height of the free surface; h is the flow depth; θ_x and θ_y are the angle of inclination at the bed along the x and y directions respectively; α and β are the momentum correction factors; $\upsilon = \mu/\rho_d$ is kinematic viscosity, ρ_d is the equivalent density of the debris mixture, and $\rho_d = \rho_s \mathrm{v_s} + \rho_w \mathrm{v_w}$, ρ_s and ρ_w are the densities of solid grains and water, $\mathrm{v_s}$ and $\mathrm{v_w}$ are the volumetric concentrations of solids particles and water in the mixture; and $\tan\xi$ is the dynamic friction coefficient.

NUMERICAL SOLUTION

Digital Elevation Models (DEM) in GIS automatically extract topographic variables, such as basin geometry, stream networks, slope, aspect, flow direction, etc. from raster elevation data. Three schemes for structuring elevation data for DEMs are: triangulated irregular networks (TIN), grid networks, and vector or contour-based networks (Moore et al., 1991). The most widely used data structures are grid networks with rows and columns where each cell contains a value representing information, such as elevation. The grid-based map of the studied area is immensely useful for numerical solution of the partial differential equations governing the propagation of debris flows. Finite-difference method on rectangular grids is widely used in numerical models of environmental flows. Therefore, in this paper, we used grid networks in GIS as the rectangular grids of finite-difference methods.

In a raster-based DEM analysis, each cell has eight possible flow directions (left, right, up, down, plus the four diagonals), as show in Fig. 10a. The flow direction of a cell is expressed in degrees: left=0, up=90, right=180, down=270; and the diagonals: 45, 135, 225, 315. Within a cell overland flow is routed along one flow direction. The flow direction is the maximum downslope direction which is determined form the raster-based DEM (Fig. 10b). The numerical solution is achieved using a finite difference formulation based on the DEM grid. For a general two-dimensional computation, as shown in Fig. 11, the finite difference equations are:

The continuity equation

$$\frac{h_{i+1/2,j+1/2}^{n+3}-h_{i+1/2,j+1/2}^{n+1}}{2\Delta t}+\frac{M_{i+1,j+1/2}^{n+2}-M_{i,j+1/2}^{n+2}}{\Delta x}+\frac{N_{i+1/2,j+1}^{n+2}-N_{i+1/2,j}^{n+2}}{\Delta y}=0 \tag{7}$$

And the momentum equation of x-component

$$\frac{M_{i,j+1/2}^{n+2}-M_{i,j+1/2}^{n}}{2\Delta t}+\frac{\alpha}{\Delta x}\left[\frac{\left(M_{i+1,j+1/2}^{n}+M_{i,j+1/2}^{n}\right)^2}{4h_{i+1/2,j+1/2}^{n+1}}-\frac{\left(M_{i,j+1/2}^{n}+M_{i-1,j+1/2}^{n}\right)^2}{4h_{i-1/2,j+1/2}^{n+1}}\right]$$

$$+\frac{\alpha}{\Delta y}\left[\frac{\left(M_{i,j+1/2}^{n}+M_{i,j+3/2}^{n}\right)\left(N_{i+1/2,j+1}^{n}+N_{i-1/2,j+1}^{n}\right)}{h_{i-1/2,j+1/2}^{n+1}+h_{i+1/2,j+1/2}^{n+1}+h_{i+1/2,j+3/2}^{n+1}+h_{i-1/2,j+3/2}^{n+1}}-\frac{\left(M_{i,j+1/2}^{n}+M_{i,j-1/2}^{n}\right)\left(N_{i+1/2,j}^{n}+N_{i-1/2,j}^{n}\right)}{h_{i-1/2,j-1/2}^{n+1}+h_{i+1/2,j-1/2}^{n+1}+h_{i+1/2,j+1/2}^{n+1}+h_{i-1/2,j+1/2}^{n+1}}\right]$$

$$=-g\frac{\left(h_{i+1/2,j+1/2}^{n+1}+h_{i-1/2,j+1/2}^{n+1}\right)\left(H_{i-1/2,j+1/2}^{n+1}-H_{i-1/2,j+1/2}^{n+1}\right)}{2\Delta x}+$$

$$\upsilon\beta\left[\frac{M_{i-1/2,j+1/2}^{n}-2M_{i+1/2,j+1/2}^{n}+M_{i+3/2,j+1/2}^{n}}{\left(\Delta x\right)^2}+\frac{M_{i,j-1/2}^{n}-2M_{i,j+1/2}^{n}+M_{i,j+3/2}^{n}}{\left(\Delta y\right)^2}\right]$$

$$-\cos\theta_x\tan\varphi\sqrt{g\frac{h_{i+1/2,j+1/2}^{n+1}+h_{i-1/2,j+1/2}^{n+1}}{2}} \qquad (8)$$

An analogous finite difference expression represents the momentum equation of y-component in (6).

SIMULATION OF THE REAL DEBRIS FLOW

The above approach is used to simulate the real debris flow that occurred at Minamata-Hougawachi. In this simulation, the depth of the landslide mass is assumed as the initial thickness of flow and the rheological parameters are set constant throughout the duration of the flow event (Tab. 2). A time-lapse simulation of the dynamic progression and deposition of the debris flow over the 3-dimensional terrain is illustrated in Fig.12. The simulation results show that it took about 200 seconds to travel 1500 m along the channel, and an average flow velocity is about 7.5 m/s. The affected region can be dynamically displayed again at different time.

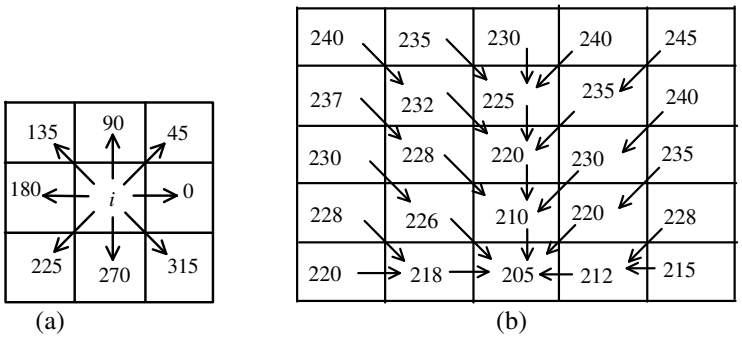

Fig.10 Flow direction (a: possible flow direction in a cell; b: flow direction in a DEM)

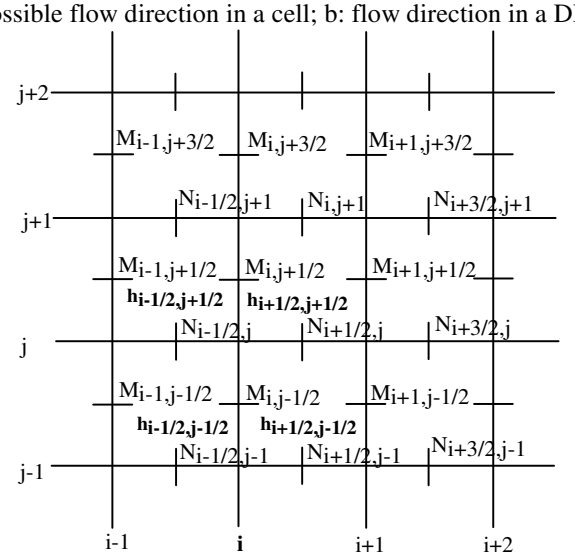

Fig.11 Grids for 2-dimensional debris flow computation

Tab.2 Material properties and rheological parameters for simulation

ρ(kg/m^3)	α	β	μ(Pa·s)	g(m/s^2)	$\tan\xi$
2200	1.25	1.0	0.11	9.8	0.6

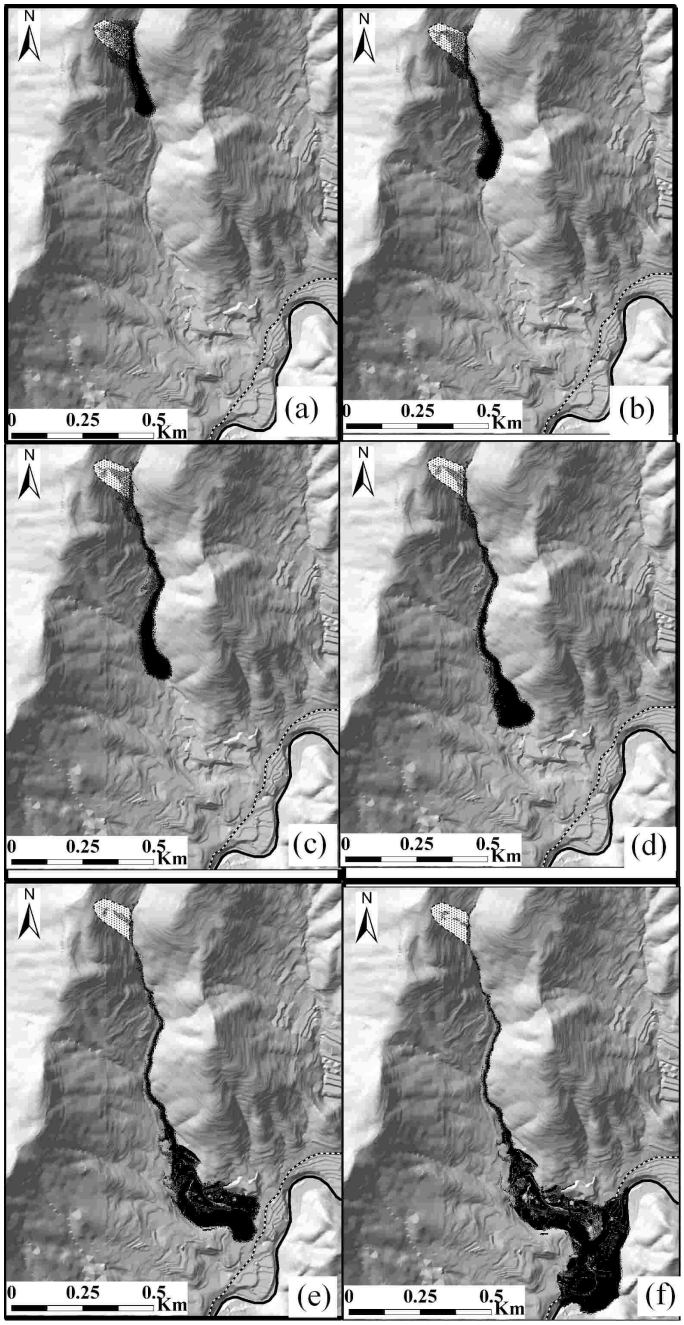

Fig.12 Simulation of debris flow propagation in region of the actual Minamata-Hougawachi region debris flow (a: 30s; b: 60s; c: 90s; d: 120s; e: 180s; f: 220s)

DEBRIS FLOW HAZARD MAP

Assuming the pattern of landslide disasters in the Minamata-Hougawachi region is the same as the landslide of July 20, 2003, namely, the slope sliding mass combining with the mountain torrent forms a debris flow passing along the stream valley, five stream valleys that are the most likely to be affected by these processes are recognized. For each stream valley, there are several potential landslides areas upriver. Because they are unlikely to fail at the same time, only one potential landslide was selected to simulate the inundated area for each stream valley (cases 1-5, numbered in Fig. 9). Case 1 (Fig. 9) is the real debris flow and has been simulated in the above section. Using the

parameters calibrated by the historic landslide, four debris flows from the unstable slope units are simulated (cases 2-5). For these simulations, the flow times and distances are listed in Tab. 3, and the propagation processes of the debris flows is illustrated in Fig. 13. Finally, the debris flow hazard zones are mapped in Fig. 14, in which the inundated areas of the debris flows, the potentially affected houses and road sections are shown.

Tab.3 Flow time and distance for case 2-5

	Case 2	Case 3	Case 4	Case 5
Time(s)	160	180	100	50
Distance(m)	1100	1300	700	400
Average velocity(m/s)	6.9	7.2	7.0	8.0

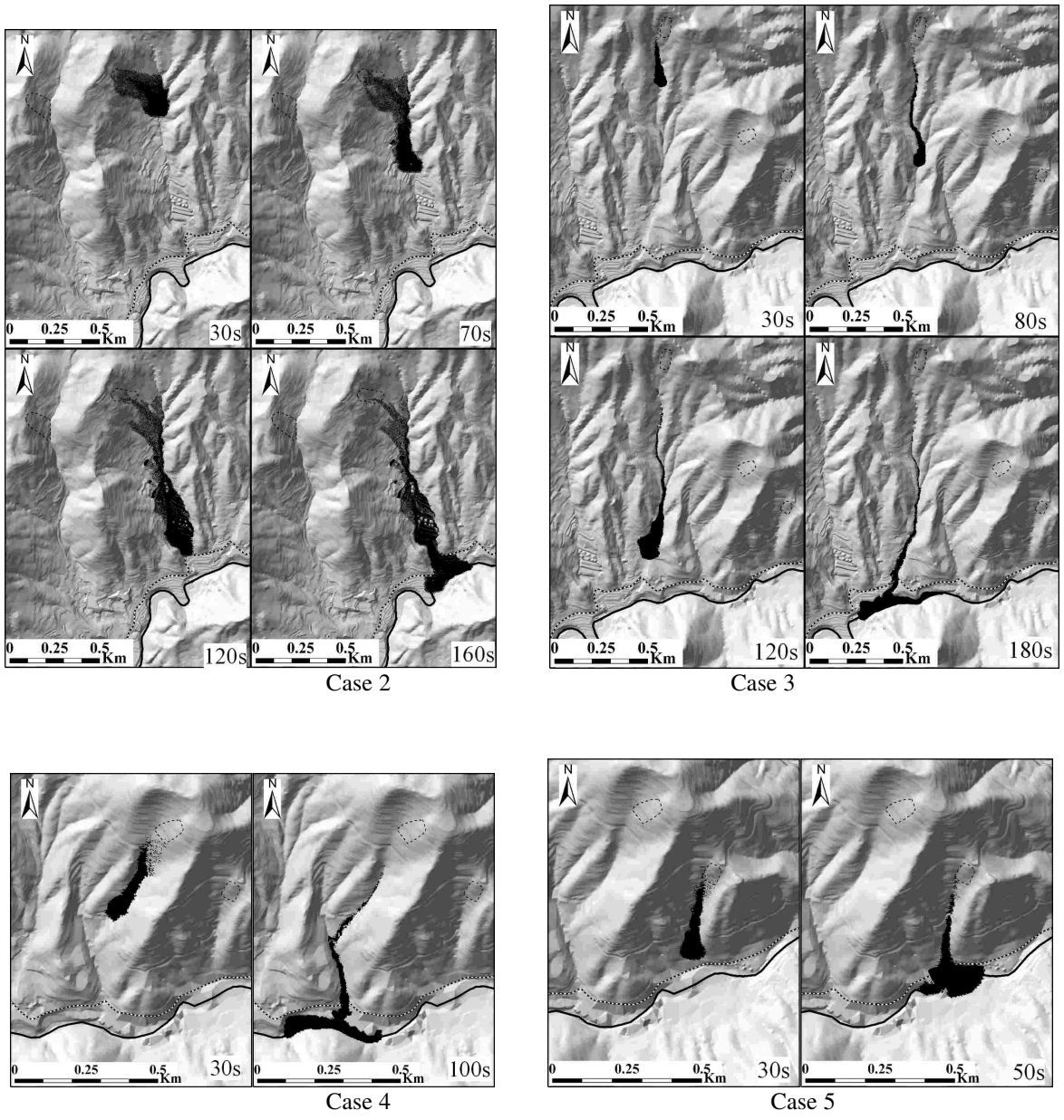

Fig.13 Inundated areas of simulated potential debris flows (cases 2-5)

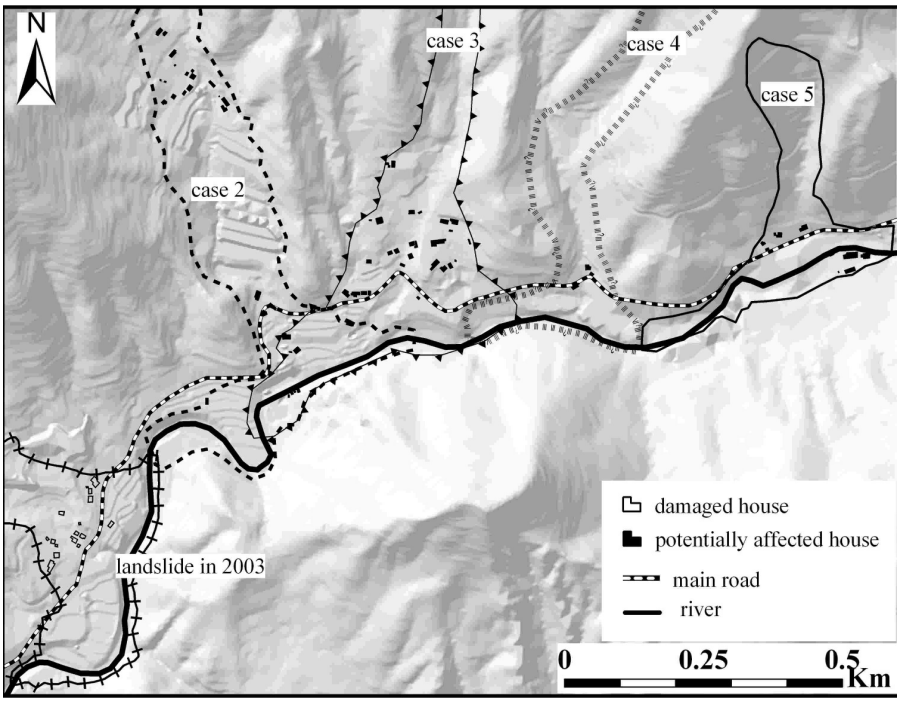

Fig.14 Landslide hazard map with distribution of houses, river and road

CONCLUSIONS

The field survey following July 20, 2003 disaster in the Minamata-Hougawachi region of Kumamoto Prefecture provides an insight into typical landslide mechanisms of the study area. Where map unit An-5 is overlain by map unit An-7 appears prone to landslide, particularly during high-intensity rainfall events during which the rainwater can seep within the seriously weathered An-7. When the pore water pressure develops at the contact of the impermeable An-5, a landslide may potentially occur along the interface between An-7 and An-5.

Based on the study of the landslide of July 20, 2003, the parameters for 3D slope stability analysis are back calculated. To locate the potential landslides, the study area is divided into slope units using the hydrologic analysis tool in ArcGIS, and using the GIS-based of the 3D limit equilibrium model for slope stability analysis, the location of potential landslides are obtained.

Most of the debris flows originally occur in the form of rainfall-induced landslides before they move into the valley channel. In order to define a debris flow safety zone, the key requirements consist of the predication of the flow trajectory over the complex topography, the potential debris flow run out distance, and the inundation area. In this paper, a depth-averaged two-dimensional numerical model incorporating GIS is used to model the propagation of the debris flow designed to emulate the historic debris flow. We also use this simulation procedure to model potential landslides that might form debris flows in other stream valleys in the Minamata-Hougawachi region. Using the parameters calibrated by the past landslide, four debris flows from unstable slope units are simulated (cases 2-5). According to the results of debris flow simulation, the potentially inundation area is modeled, mapping the potentially affected houses, streams and roads. Since the actual inundated areas are controlled by the volume of the landslide mass, the rainfall amount, and the regional terrain following any actual landslide, there can be some uncertainties when forecasting the affected areas in this study. The two-step procedrue for hazard predition and assessment of landslide and debris flow allows many model runs to be performed and scenarios based on many different events occurring in many locations could be developed.

REFERENCES

Anderson S.A. (1995). Analysis of Rainfall-induced debris flows. Journal of Hydraulic Engineering 121:544-552.

Carrara A., Cardinali M., Detti R., Guzzetti F., Pasqui V., Reichenbach P. (1991). GIS techniques and statistical models in evaluating landslide hazard. Earth Surface Process and Landforms 16:427-445.

Chen H., Lee C.F. (2000). Numerical simulation of debris flows. Canadian Geotechnical Journal 37:146-160.

Dai F., Lee C.F., Wang S. (1999). Analysis of rainstorm-induced slide-debris flows on natural terrain of Lantau Island, Hong Kong. Engineering Geology 51:279-290.

David R.M. (2002). Arc Hydro: GIS for water resources. ESRI Press, Redlands, CA, USA.

Denlinger R.P., Iverson R.M. (2001). Flow of variably fluidized granular masses across three-dimensional terrain. Journal of Geophysical Research 106:553-566.

Dymond J.R., Derose R.C., Harmsworth G.R. (1995). Automated mapping of land components from digital elevation data, Earth Surfure Processes and Landforms 20:131-137.

Fiorillo F., Wilson R.C. (2004). Rainfall induced debris flows in pyroclastic deposits, Campania (southern Italy). Engineering geology 75:263-289.

Fleming R.W., Ellen S.D., Algus M.A. (1989). Transformation of dilative and contractive landslide debris into debris flow - An example from Marin Country, California. Engineering Geology 27: 201-223.

Ghilardi P., Natale L., Savi F. (2001). Modeling Debris Flow Propagation and Deposition. Physics and Chemistry of the Earth 26: 651-656.

Hansen A. (1984). Landslide hazard analysis. In: Brunsden D., and Prior D.B., (Editors), Slope instability. Wiley, New York, 523-602.

Hungr O. (1995). A model for the runout analysis of rapid flow slides, debris flows and avalanches. Canadian Geotechnical Journal 32(4): 610-623.

Hunt B. (1994). Newtonian fluid Mechanics treatment of debris flows and avalanches. Journal of Hydraulic Engineering 120: 1350-1363.

Iwao Y. (2003). Slope hazard induced by heavy rain in 2003, Minamata City, Kumamoto. Journal of the Japan Landslide Society 40:239-240. (in Japanese)

Laigle D., Coussot P. (1997). Numerical modeling of Mudflows, Journal of Hydraulic Engineering 123: 617-623.

Mainali A., Rajaratnam N. (1994). Hydraulics of debris flows. Journal of Hydraulic Engineering 120:104-123.

Moore I.D., Grayson R.B., Ladson A.R. (1991). Digital terrain modeling: a review of hydrological, geomorphological and biological applications. Hydrological Processes 5:3-30.

O'Brien J.P., Julien P.J., Fullerton W.T. (1993). Two-dimensional water flood and mudflow simulation. Journal of Hydraulic Engineering 119:244-261.

Takahashi T., Nakagawa H., Harda T., Yamashiki Y. (1992). Routing debris flows with particle segregation. Journal of Hydraulic Engineering 118:1490-1507.

Taniguchi Y. (2003). Debris disaster caused by local heavy rain in Kyushu area on July 20th, 2003 (prompt report), Minamata debris disaster. Journal of the Japan Society of Erosion Control Engineering 56:31-35. (in Japanese)

Wen B.P., Aydin A. (2005). Mechanism of a rainfall-induced slide-debris flow: Constraints from microstructure of its slip zone. Engineering Geology 78:69-88.

Wang C., Li S., Esaki T. (2008). GIS-based two-dimensional numerical simulation of rainfall-induced debris flow. Natural Hazards and Earth System Sciences 8(1):47-58.

Xie M., Esaki T., Zhou G., Mitani Y. (2003). Geographic information systems-based three-dimensional critical slope stability analysis and landslide hazard assessment. Journal of Geotechnical and Geoenvironmental Engineering, ASCE, 129:1109-1118.

Xie M., Esaki T., Qiu C., Wang C. (2006). Geographical information system-based computational implementation and application of spatial three-dimensional slope stability analysis. Computers and Geotechnics 33(4-5): 260-274.